433 MHz implantable wireless stimulation of spinal nerves

J. P. Carmo, J. C. Ribeiro, J. F. Ribeiro, M. F. Silva, P. M. Mendes, and J. H. Correia

University of Minho, Dept. Industrial Electronics

Guimaraes, PORTUGAL, **jcarmo@dei.uminho.pt**

Abstract - **This paper presents a implantable wireless microsystem concept for operation in the 433 MHz ISM band. The proposed microsystem is composed by two independent subsystems: the electrostimulation and the radio-frequency (RF) subsystems. The electrostimulation part is a silicon box with groves to pass the nerves to be stimulated. The cover of the silicon box contains electrodes for electrical contacting with the nerves. Wafer-level packaging (WLP) techniques will allow the joining of the RF and the electrostimulation subsystems. The target of this implantable microsystem is for RF reception at 433 MHz of user commands to activate the micturition function and the erection (on males) patients. The expected microsystem area will be of 5×5mm^2.**

Keywords - **Implantable devices, RF transceivers, CMOS.**

I. INTRODUCTION

This paper presents an implantable wireless microsystem to stimulate the nerves of spine according the desire of the patient. The mitriction and penian erection (in the case of males) can be induced by pressing a push-button for nerve excitation. The electrostimulation commands must be sent by radio-frequency (RF) transmission at the frequency of 433 MHz for avoiding the use of wires to connect the electrostimulator to the patient's control. This last solution is the one that is adopted for several years with relative success, but with the drawback to use wires (which can break of decrease the patient's freedom and comfort).

II. IMPLANTABLE DEVICES FOR ELECTRICAL STIMULATION

The Figure 1 shows the commonly adopted system architecture used to control the inferior urinary system. The system contains a signal generator to generate the appropriate stimulus to activate, e.g., the bladder. This stimulus is transmitted to the external coil, which induces the signal in the internal coil. Reaching the biologic environment, a receiver module delivers the stimulus trough the transmission cables that carry the signal to the cuff electrode. Since the internal coil is placed in the frontal region and the electrodes are in the back, the transmission cables must go through the body and are one main cause of system failure. Moreover, the existence of these cables requires a small opening in the duramater, not good for the spinal cord integrity. One main benefit of the microsystem approach is the possibility to avoid cables trespassing the duramater. A wireless solution is more suitable and thus, a RF receiver with good sensitivity is necessary. This paper presents a wireless solution for this biomedical application.

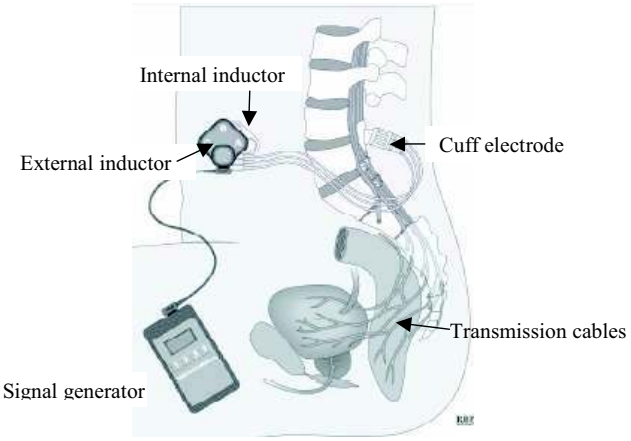

Fig. 1: Schematic view of the overall system used for bladder control.

III. THE IMPLANTABLE MICROSYSTEM

A. System architecture of the wireless microsystem

The increased demand for reducing the failure associated with long wires and the associated risk of infection or shifts in the wires is pushing the researchers to find new solution for applying microtechnologies. Also, and not less important is the internment period associated with the surgical intervention. Due to the highly invasive intervention that is required using the traditional technique, the patients, even when there are no complications are required to stay a few days in the hospital. The availability of a device to allow a less invasive method would be more comfortable for the patient, reducing also the hospital costs associated to the surgery.

The new devices based on RF must be small enough to fit inside the spinal cord; it must be able to deliver the required stimulus (power and timing) and it must be possible to communicate with the device using a RF signal. This requires a fully integrated microsystem (with sensors, RF systems and integrated antennas). The antenna integration requires the availability of an electrically small antenna fabricated on materials compatible with the fabrication of integrated circuits. This integration requires the use of wafer-level packaging (WLP) techniques.

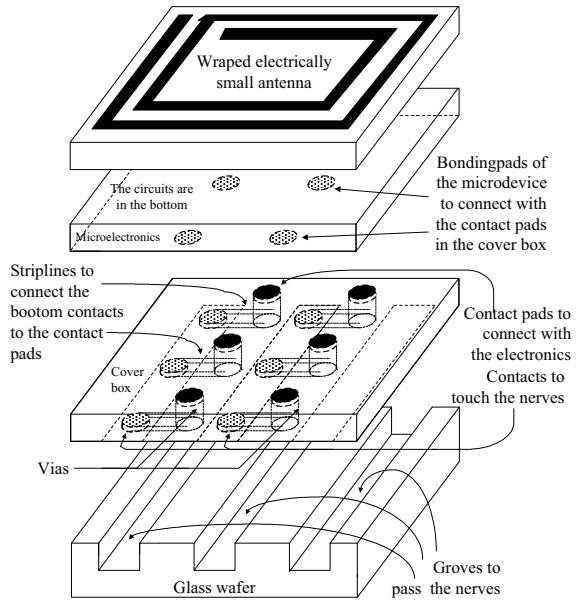

Fig. 2: An artist impression of the complete implantable microsystem.

As depicted in Figure 2, the electrostimulation part is a box made of a silicon wafer with opened/etched groves to pass the nerves for stimulation. Above the stimulation box is putted a cover containing electrodes that make electrical contact with the nerves, while at the same time are connected by a thin set of vias to pads placed in the opposite side. The solid-state circuits part that comprise the microelectronics of control and the RF transceiver as well as the associate antenna, are placed upside the cover, by using WLP techniques for such a purpose.

B. The operation frequency

The selection of a suitable frequency in an implantable device is not an easy task because the devices must present the minimum sizes for in-vivo placement. Thus, small (and smaller than the wavelenght) antenas must be used to not compromise the miniaturisation. Previous works of biomedical applications at the frequency of 2.4 GHz [2], and the investigation of new frequencies [3] and new geometries [4] made possible to have smaller antennas to integrate in wireless microsystems [5][6]. This makes the selection of the most suitable frequency, one of the more decisive aspects in the design of RF transceivers. Normally, the desired range, baud-rate and power consumptions trade between them and with the frequency of operation. The range is limited by the usable frequency and, in the context of implantable devices, the skin depth decreases with the frequency. Thus, to keep or even to increase the range an increase in the transmitted power must be made. However, such an increase can not be acceptable in implantable devices. Taking in account the electrical constants for the human tissue where the device will be implanted, e.g., cortical bone (ε_r, of 13.77 and an electrical conductivity, σ, of 0.1032 S.m^{-1}) and considering the skin-depth, $\delta=\{2\pi 10^9 . f_{GHz}\times(\mu_0\varepsilon_0\varepsilon_r/2[1+(18\sigma/f_{GHz})^2]^{-1/2})^{-1/2}\}^{-1}$ [m], where $\varepsilon_0=10^{-9}/(36\pi)$ F.m^{-1}, $\mu_0=4\pi 10^{-7}$ H.m^{-1}, are the electric permitivity and the magnetic permeability for the free-space, respectively. The quantity f_{GHz} is the RF frequency expressed in giga-cycles per second. The table I presents the values of the skin-depth for three of the most used frequencies for possible usage bands and the respective losses for two key-distances: for the skin-depth and for 20 cm. This last distance was selected because it correspond to the worse case in terms of wireless communication distance for the proposed implantable wireless microsystem. The frequency of 433 MHz presents the less and the still acceptable losses. This means that the loss correspondent to a penetration of 20 cm in the human-body is equivalent to an equivalent loss in the free-space for a distance of 14 meters. Thus, a RF transceiver designed for short-range communications at this frequency [7] is suitable for use as RF part in the proposed implantable microsystem.

TABLE I: SKIN-DEPTH, δ[mm] AND LOSSES [dB] FOR δ AND FOR 20 cm.

Frequency	Skin-depth δ[mm]	Loss $L_1(\delta)$ [dB]	L_2(20 cm) [dB]
2.4 GHz [2]	5.0383 mm	4.3429	172.4
5.7 GHz [5]	2.2287 mm	4.3429	389.7
433 MHz [7]	18.0759 mm	4.3429	48.1

IV. RF TRANSCEIVER AT 433 MHZ

A. Architecture

It was fabricated a RF transceiver for operation at the frequency of 433 MHz, with ASK (Amplitude Shift Keying) modulation in the OOK (On/Off Keying) variant, using the AMIS 0.7 µm CMOS process (with two metals and one polysilicon layer). The Figure 5 shows the block-diagram of the RF transceiver, and as it can be seen, the 433 MHz carrier frequency is generated by a Phase-Locked Loop (PLL) in the transmitter section. The reference signal is generated by a crystal oscillator working at 13.56 MHz.

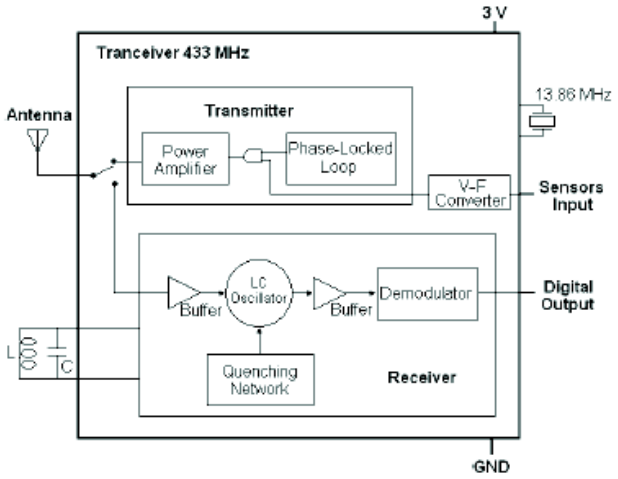

Fig. 5: The RF transceiver structure.

B. RF receiver

The receiver was implemented with super-regenerative architecture [8][9] in order to maximise its sensitivity. As depicted in the same figure, the receiver includes na oscillator, two buffers, a quenching amplifier and an envelope detector as OOK demodulator. The quenching network supervises the super-regeneration phenomena and the output of the receiver is transmitted through a bit stream. The Figure 6 shows the schematic of the antenna front-end subsystem of the receiver. The selected topology for the *LC* oscillator was of complementary cross-coupled type with a dual pair of n- and p-type MOSFETs. The MOSFETs M_1, M_2, M_3 and M_4 provide the negative resistance effect, R_{neg} [Ω], The parallel pair of passive components composed by the capacitor C [F] and by the inductance L [H] provide the feedback between the two pairs of MOSFETs M_1/M_2 and M_3/M_4.

The MOSFET M_5 uses the reference voltage V_{ref1}=0.93 V to limit the bias current to 10 μA, while the MOSFET M_6 (a part of the quenching circuit) is controlled by the signal V_{quench} to switch on and off the *LC* oscillator. The passive components of the *LC* oscillator are selected to have a resonant frequency of 433 MHz. A transmission gate (synchronized with the quenching signal) is used to short-cut the two output terminals of the *LC* oscillator during its disabling for decreasing the extinction time of the oscillations. A cascade current source is used to couple the RF signal from the antenna to the *LC* oscillator. Thanks to the cascade topology, the backward isolation is high, thus the coupling of the oscillatory signals into the antenna is low. In this sequence of ideas, the receiver contains an output buffer to isolate the *LC* oscillator from the rest of the receiver in order to minimize the load effect and to not interfere with the correct operation of the oscillator (e.g., minimizing the contribution for the phase and frequency noise in the generated oscillations). This buffer is a differential source follower to minimize the attenuation of the oscillatory signal – see the Figure 7.

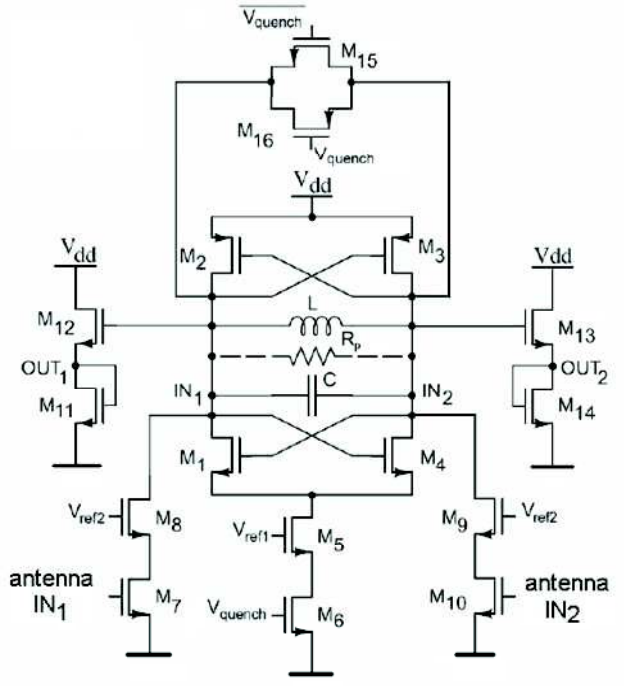

Fig. 6: The schematic of the antenna front-end subsystem of the receiver.

The differential topology was selected due to its improved noise immunity. A differential-to-single-ended conversion circuit is needed to connect this oscillator to the envelope detector. As illustrated in the Figure 6, such a purpose is achieved with a differential amplifier (with the OUT_1/OUT_2 inputs and the V_{single} output). The voltages at the inputs of the differential amplifier are $V_1=V_{CM}+V_{RF}(t)$ and $V_2=V_{CM}-V_{RF}(t)$, whose common mode voltage, V_{CM} [V], must be such that $V_{CM} \leq V_{dd}-I_{ds(M23)}.R_1-V_{th}$ for saturating all the MOSFETs.

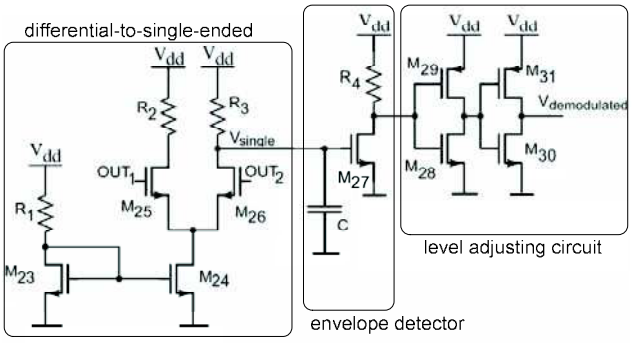

Fig. 7: The schematic circuit of the demodulator, which is composed by a differential-to-single-ended converter, by an envelope detector and by a level adjusting circuit.

C. RF transmitter

The RF transmitter is composed of a crystal-controlled PLL and a switched class E power amplifier (PA). The PA is a high-efficiency switching amplifier based on a NMOS transistor as switch RF switch, and a load network (L_{DC}, C_1, C_2, and L) that avoids the simultaneous imposition of significant voltage and current on the switch [10][11], thus yielding an highly efficient operation. The FSK (Frequency Shift Keying) and PSK (Phase Shift Keying) modulations presents less bit error probabilities (BEP or P_e), when compared with the ASK modulation. However, due to the simplicity of the ASK modulation and the possibility that offers to ensure a compatibility with other commercial modules, made this the adopted modulation. Moreover, the ASK modulation requires a less channel bandwidth than PSK or FSK. The use of the ASK in the OOK variant where the carrier is switched on and off, the PLL circuit can be relaxed. Thus, and to ensure carrier stability, the PLL is of integer division ration in the feedback, with a crystal reference oscillator of 13.56 MHz. The crystal oscillator unit provide both the carrier signal, by way of multiplying the 13.56 MHz reference signal by thirty-two in the PLL, and to provide the quench signal - by dividing it by eight - e.g., a quenching frequency of only 1695 kHz.

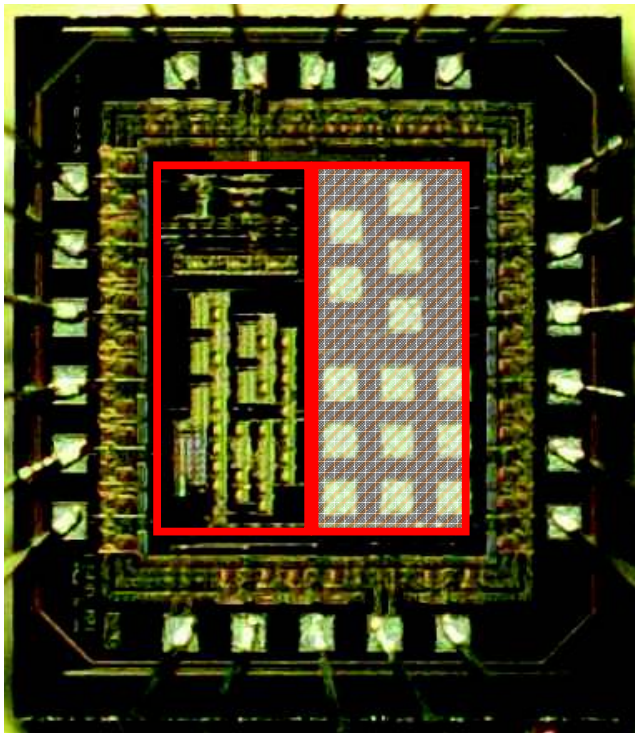

Fig. 8: A first prototype of the RF transceiver at 433 MHz.

IV. CONCLUSIONS

This paper presented a wireless implantable microsystem for operation in the 433 MHz ISM band, and for use in urology. The electrostimulation part of the microsystem is a box made in a silicon wafer with groves for passing the nerves for stimulation. Above the box, a cover containing electrodes make electrical contacts with the nerves to be stimulated. Using wafer-level packaging (WLP) techniques, the part that contains the electronics and the antenna are joined together with the electrostimulation part. This implantable microsystem allows the user to send commands to activate the micturition function and the erection (on male). The microsystem has an area of 5×5mm^2. Further details about the design and fabrication of the stimulation part can be obtained in [12]. To finish, the Figure 8 shows a photograph of the first prototype of the fabricated RF transceiver with a super-regenerative receiver for improved sensitivity. The RF transceiver was fabricated in the AMIS 0.7 μm CMOS process. The right-sided shaded area (with internal test-pads and photodiodes) doesn't belong to the RF transceiver.

REFERENCES

[1] R. A. Gaunt, A. Prochazka, "Control of urinary bladder function with devices: successes and failures," Progress in Brain Research, Elsevier, Vol. 152, pp. 163-194, 2005.

[2] J. P. Carmo, *et al*, "A 2.4-GHz Low-Power/Low-Voltage Wireless Plug-and-Play Module for EEG Applications", IEEE Sensors Journal, Vol. 7, No. 11, pp.1524-1531, full paper in Acrobat PDF, November 2007.

[3] P. M. Mendes, *et al*, "Analysis of chip-size antennas on lossy substrates for short-range wireless microsystems", in Proc. SAFE 2002, pp. 51 54, Veldhoven, The Netherlands, November 2002.P. Mendes, *et al*, "Integrated chip-size antennas for wireless microsystems: Fabrication and design considerations", Journal of Sensors and Actuators - A, Vol. 125, pp. 217-222, January 2006.

[4] F. Touati, M. Pons, "On-chip integration of dipole antenna and VCO using standard BiCMOS technology for 10 GHz applications", in Proc. 29th ESSCIRC, pp. 493-496, Estoril, Portugal, September 2003.

[5] J. Carmo, *et al*, "5.7 GHz on-chip antenna/RF CMOS transceiver for wireless sensors", Journal of Sensors and Actuators - A, Vol. 132/1, pp. 47-51, ScienceDirect, November 2006.

[6] J. L. Volakis, "Antenna Engineering Handbook", 4th Edition, McGraw-Hill Professional, 2007.

[7] J. C. Ribeiro, *et al*, "Wireless interface for sensors in smart textiles", in Proc. Eurosensors XIX, pp. TC2.1-2, Barcelona, Spain, 2005.

[8] A. Vouilloz, *et al*, "A low-power CMOS super-regenerative receiver at 1 GHz", IEEE Journal of Solid-State Circuits, Vol. 36, No. 3, pp. 440-451, March 2001.

[9] N. Joehl, *et al*, "A low-power 1-GHz super-regenerative transceiver with time-shared PLL control", IEEE Journal of Solid-State Circuits, Vol. 36, No. 7, pp. 1025-1031, July 2001.

[10] N.O. Sokal, A.D. Sokal, "Classe E - a new class of high-efficiency tuned single-ended switching power amplifiers, IEEE Journal of Solid State Circuits, Vol. 10, No. 3, pp. 168–176, 1975.

[11] R. Morais, *et al*, "A wireless RF CMOS mixed-signal interface for soil moisture measurements", Journal of Sensors and Actuators - A, Vol. 115, pp.376-384, September 2004.

[12] J. P. Carmo, *et al*, "A New Implantable Wireless Microsystem to Induce Mictrition in Spinal Injury Patients", in Proc. 15th IEEE Mediterranian Electromechanical Conference - MELECON 2010, pp. 389-392, La Valletta, Malta, 25-28 April 2010.